A Mutation Linked with Bartter's Syndrome Locks Kir 1.1a (ROMK1) Channels in a Closed State

Thomas P. Flagg,* Margaret Tate,* Jean Merot,‡ and Paul A. Welling*

From the *Department of Physiology, University of Maryland School of Medicine, Baltimore, Maryland 21201; and ‡Department de Biologie Cellulaire et Moleculaire, Centre d'Etudes Saclay, Gif sur Yvette, France 91191

abstract Mutations in the inward rectifying renal K^+ channel, Kir 1.1a (ROMK), have been linked with Bartter's syndrome, a familial salt-wasting nephropathy. One disease-causing mutation removes the last 60 amino acids (332–391), implicating a previously unappreciated domain, the extreme COOH terminus, as a necessary functional element. Consistent with this hypothesis, truncated channels (Kir 1.1a 331X) are nonfunctional. In the present study, the roles of this domain were systematically evaluated. When coexpressed with wild-type subunits, Kir 1.1a 331X exerted a negative effect, demonstrating that the mutant channel is synthesized and capable of oligomerization. Plasmalemma localization of Kir 1.1a 331X green fluorescent protein (GFP) fusion construct was indistinguishable from the GFP–wild-type channel, demonstrating that mutant channels are expressed on the oocyte plasma membrane in a nonconductive or locked-closed conformation. Incremental reconstruction of the COOH terminus identified amino acids 332–351 as the critical residues for restoring channel activity and uncovered the nature of the functional defect. Mutant channels that are truncated at the extreme boundary of the required domain (Kir 1.1a 351X) display marked inactivation behavior characterized by frequent occupancy in a long-lived closed state. A critical analysis of the Kir 1.1a 331X dominant negative effect suggests a molecular mechanism underlying the aberrant closed-state stabilization. Coexpression of different doses of mutant with wild-type subunits produced an intermediate dominant negative effect, whereas incorporation of a single mutant into a tetrameric concatemer conferred a complete dominant negative effect. This identifies the extreme COOH terminus as an important subunit interaction domain, controlling the efficiency of oligomerization. Collectively, these observations provide a mechanistic basis for the loss of function in one particular Bartter's-causing mutation and identify a structural element that controls open-state occupancy and determines subunit oligomerization. Based on the overlapping functions of this domain, we speculate that intersubunit interactions within the COOH terminus may regulate the energetics of channel opening.

key words: potassium • channel • gate • subunit oligomerization • green fluorescent protein

INTRODUCTION

The inwardly rectifying K^+ channel, Kir 1.1 (ROMK), plays a critical role in kidney function (Hebert and Wang, 1997; Ho et al., 1993). Convincing correlative observations strongly support the idea that the product of the Kir 1.1 gene encodes the pore-forming subunit of particular ATP-sensitive K^+ channels that affect urine-concentrating ability and potassium homeostasis (Hebert and Wang, 1997). Indeed, immunodetectable Kir1.1 protein is restricted to the apical membrane of the thick ascending limb, distal tubule, and collecting duct (Mennitt et al., 1997; Xu et al., 1997; Kohda et al., 1998), where these unique K_{ATP} channels are exclusively expressed (Bleich et al., 1990; Wang et al., 1990a,b; Frindt and Palmer, 1989). Moreover, heterologous expression studies in *Xenopus* oocytes have revealed that Kir 1.1 exhibits nearly identical single channel conductance and high-open probability kinetics as the native secretory K^+ channel (Palmer et al., 1997). Coexpression of an ATP-binding cassette protein, cystic fibrosis transmembrane-conductance regulator, is required to confer ATP (Ruknudin et al., 1998) and glibenclamide sensitivity on Kir 1.1 (McNicholas et al., 1996; Ruknudin et al., 1998) and to recapitulate the full repertoire of native channel behavior. In these respects, the kidney secretory K_{ATP} channel has been proposed to exhibit a multimeric Kir 1.1 channel–ABC protein modifier subunit composition, similar to the Kir 6.x/SUR channels in the heart and islet beta cells (Babenko et al., 1998).

A definitive link between the Kir1.1 gene, the renal secretory K_{ATP} channel and kidney function (Simon et al., 1996b; Karolyi et al., 1997) has been established by a familial salt-wasting nephropathy called Bartter's syndrome (Bartter et al., 1962). Resulting from genetic defects in the renal concentrating mechanism, the disorder is characterized by a constellation of fluid and electrolyte abnormalities, including polyuria, hypokalemia,

Address correspondence to Paul A. Welling, Department of Physiology, University of Maryland School of Medicine, 655 W. Baltimore St., Baltimore, MD 21201. Fax: 410-706-8341; E-mail: pwelling@umaryland.edu

J. Gen. Physiol. © The Rockefeller University Press • 0022-1295/99/11/685/16 $5.00
Volume 114 November 1999 685–700
Released online 11 October 1999
http://www.jgp.org

metabolic alkalosis, and hypotension, that resemble those observed with chronic loop-diuretic administration (Guay-Woodford, 1998). In fact, mutations within the major components of the NaCl reabsorbtive machinery in the thick ascending limb of Henle's loop have been linked with this genetically heterogenous disorder (Simon et al., 1996a,b,c; Karolyi et al., 1997). Consistent with an essential role of the secretory K_{ATP} channel in the thick ascending limb of Henle (Giebisch, 1998), loss-of-function mutations in the Kir 1.1 gene have been identified in several kindreds affected with Bartter's syndrome.

The discovery of disease-causing mutations in Kir1.1a not only provides valuable insights into the role of this channel in health and disease, it also lends illustrative clues about structural determinates of function. Like other members of the inward rectifying class of K^+ channels, a functional channel is formed by the tetrameric assembly of Kir 1.1 subunits. Each subunit is comprised of two putative transmembrane domains that flank a "P" loop containing the potassium selectivity filter and other determinants of the permeation pathway (Nichols and Lopatin, 1997). The transmembrane core is bounded cytoplasmic NH_2- and COOH-terminal domains, playing roles in channel regulation (Fakler et al., 1996; Xu et al., 1996; Choe et al., 1997; MacGregor et al., 1998), conduction (Taglialatela et al., 1994; Yang et al., 1995a) and oligomerization (Tinker et al., 1996; Koster et al., 1998). Mutations within each of these domains have been linked to Bartter's syndrome. Many of the mutations introduce nonsense codons or frameshifts in the NH_2 terminus, producing truncated proteins with obvious loss of function consequences (Simon et al., 1996b; Karolyi et al., 1997). A mutation in the core domain that alters the permeation pathway has been identified (Derst et al., 1998). Other mutations disrupt a regulatory protein kinase A phosphorylation site, Ser 219, presumably by influencing its phosphorylation state or ability to modulate channel activity (Simon et al., 1996b; Derst et al., 1997).

While no particular function has been assigned to the extreme COOH terminus of the channel, the link between a mutation that deletes the last 60 amino acids (T332–K333 frameshift) and Bartter's disease (Simon et al., 1996b) suggested an important role for this previously unrecognized domain. As predicted from the Bartter's phenotype, we found that deletion of the COOH-terminal 60 amino acid residues renders channels inactive. In the present study, we have systematically evaluated the possible functional roles of the extreme COOH-terminal domain of Kir 1.1a. By elucidating the mechanism underlying the defect, we discovered that the extreme COOH terminus acts as an obligate determinate of channel gating, maintaining the channel in a stable open state.

METHODS

cDNAs and Mutagenesis

The present study is focused on the consequences of COOH-terminal mutations in Kir 1.1. To ensure that differences in functional expression result from changes in the open reading frame (ORF)[1] rather than changes in the 3′ untranslated regions (UTR), the 3′ UTR was eliminated from wild-type rat Kir 1.1a (Ho et al., 1993) and COOH-terminal deletion mutant cDNA constructs. Mutagenesis was performed by overlap extension PCR (Ho et al., 1989). Deletion mutants (Kir 1.1a 331X, Kir 1.1a 341X, Kir 1.1a 351X, Kir 1.1a 361X, and Kir 1.1a 366X) were constructed by introducing three stop codons in frame at the appropriate locations. To create Kir 1.1a Δ332–351, a PCR product encoding amino acids 352–391 was ligated to a unique NspV site (see below). All cDNAs were subcloned between the 5′ and 3′ UTR of the *Xenopus* β-globin gene in the modified pSD64 vector to increase expression efficiency (Krieg and Melton, 1984). This vector also contains a polyadenylate sequence in the 3′ UTR ($dA_{23}dC_{30}$). Appropriate cDNA sequence was verified by dye termination sequencing (ABI Prism).

Construction of Concatemer Kir 1.1a

To critically test the dominant negative effect of Kir 1.1a 331X, three separate concatemeric cDNA constructs were created. In one construct, four wild-type Kir 1.1a subunits (4wt) were covalently linked together. The other two constructs were comprised of three wild-type subunits joined to one Kir 1.1a 331X at either the NH_2- (1mut + 3wt) or COOH- (3wt + 1mut) terminal position of the tandem tetramer.

Concatemeric Kir 1.1a constructs were generated in four steps. (a) Three separate silent mutations were engineered into Kir 1.1a to create unique restriction sites. Two of these sites, RsrII and KasI were introduced in the 5′ end of the ORF, while the other, Bpu1102I, was placed at the 3′ end. The unique 5′ sites were also introduced into the mutant Kir 1.1a 331X. (b) Two different linker oligonucleotides were independently ligated to the unique 3′ restriction site. Linker-1 encoded the 3′ end of Kir 1.1a from the Bpu1102I site (encompassing the final 14 amino acids of Kir 1.1a), codons for 10 glutamines, and the 5′ ORF of Kir 1.1a containing the unique KasI site. Linker-2 was identical to the first linker, except that it contained the unique RsrII site instead of KasI. (c) Three different dimers were constructed by linking-modified monomers together using the unique KasI site. One dimer contained two Kir 1.1a subunits with linker-2 attached to the 3′ end of the ORF. The second dimer contained an RsrII site at the 5′ end of the ORF, but no 3′ linker. The third dimer was identical to the second except that the 3′ subunit encoded the mutant, Kir 1.1a 331X. (d) To create the tetrameric concatemers, dimers were linked together using the unique RsrII site. One concatemer contained four wild-type subunits artificially linked together (4wt), while the other contained three wild-type subunits ligated to a single mutant (3wt + 1mut).

To generate the third concatemer (1mut + 3wt), a similar stepwise approach was adopted. (a) A silent mutation containing an NspV site was introduced into Kir 1.1a at the codons for amino acids 331–332. (b) Linker-3 encoding the unique NspV site, residue 331 of Kir 1.1a, codons for 10 glutamines, and the 5′ ORF of Kir 1.1a containing the unique KasI site was ligated on to the unique NspV-restriction site. (c) A dimer was generated by ligating a modified Kir 1.1a monomer containing linker-2 (as above)

[1]*Abbreviations used in this paper:* EGFP, enhanced green fluorescent protein; mut, mutant; ORF, open reading frame; wt, wild type.

to the construct containing linker-3 using the unique KasI site. (d) Two dimers were joined as before to create the tetrameric concatemer with Kir 1.1a 331X at the extreme 5′ position in the ORF, followed by three wild-type subunits (1mut + 3wt).

The sequence of each modified monomer was confirmed by dye termination DNA sequencing. Appropriate tetrameric construction was confirmed by restriction enzyme analysis. Moreover, in vitro transcription from each concatemeric cDNA template yielded cRNA transcripts of the correct size.

Construction of Green Fluorescent Protein Fusion Proteins

To assess the cellular distribution of Kir 1.1a and Kir 1.1a 331X, the ORF of enhanced green fluorescent protein (EGFP; Clontech) was ligated, in frame, to the 5′ end of the open reading frame of either Kir 1.1a or Kir 1.1a 331X. EGFP (GFPmut1) is a mutated form of the *Aequoria victoriae* protein, GFP, that contains two amino acid substitutions in the chromophore region (F64L and S65T) and uses preferred human codons. It exhibits single excitation and emission peaks at 490 and 509 nm, respectively, fluorescing 35× more intensely than wild-type GFP when excited at 488 nm (Cormack et al., 1996). EGFP was subcloned into the modified pSD64 for use as a cytosolic marker.

cRNA Synthesis

Complementary RNA was transcribed in vitro in the presence of capping analogue G(5′)ppp(5′)G using PstI or SmaI linearized cDNA templates. SP6 RNA polymerase was used in all reactions (mMESSAGE mMACHINE; Ambion Inc.). After DNaseI treatment, cRNA was purified by phenol-chloroform extraction and ammonium acetate/isopropanol precipitation. Yield and concentration were measured spectrophotometrically and confirmed by agarose gel electrophoresis.

Oocyte Isolation and Injection

Female *Xenopus laevis* frogs were obtained from NASCO. Standard protocols were followed for the isolation and care of *X. laevis* oocytes. In brief, frogs were anesthetized by immersion in 0.15% 3-aminobenzoate and a partial oophorectomy was performed through an abdominal incision. Oocyte aggregates were manually dissected from the ovarian lobes, and then incubated in a calcium-free ORII medium (82.5 mM NaCl, 2 mM KCl, 1 mM MgCl2, and 5 mM HEPES) containing collagenase (type IA, 2 mg/ml; Sigma Chemical Co.) for ~2 h at room temperature to remove the follicular layer. After oocytes were washed extensively with collagenase-free ORII, they were placed in a modified L15 medium (50% Leibovitz's medium, 10 mM HEPES, pH 7.4) and stored at 19°C. 12–24 h after isolation, healthy-looking Dumont stage V–VI oocytes were pneumatically injected (PV820 picopump; World Precision Instruments, Inc.) with 50 nl of water containing 0–50 ng of cRNA, and then stored in L15 medium at 19°C. Channel activity was assessed 2–6 d after injection.

Confocal Microscopy and Image Analysis

Laser-scanning confocal microscopy was used to determine the cellular localization of EGFP-Kir 1.1a and EGFP-Kir 1.1a 331X. Whole, unfixed oocytes bathed in ORII solution were visualized through a APOCHROMAT 10× objective lens (NA = 0.45; Carl Zeiss, Inc.) using an LSM410 microscope (excitation with 488 nm line of an Omnichrome series 643 Kr/Ar ion laser; Carl Zeiss, Inc.). Fluorescent emissions were passed through a 515-nm long pass filter. Background autofluorescence exhibited by uninjected oocytes was calibrated to zero by adjusting brightness and contrast settings at a constant pinhole size. These settings were maintained throughout the course of studies. Plasma membrane delimited fluorescence was quantified at equatorial focal sections of oocytes using Image software (National Institutes of Health). Average plasmalemmal pixel intensity was determined for continuous line segments of fixed width (~3 μm) drawn around the entire circumference of the oocyte. For all images, pixel intensity was within the linear range as assessed by histogram analysis for each cRNA dose. At least six cells from two donors were analyzed for four to five cRNA injection doses.

Electrophysiology

Whole cell oocyte currents were monitored using a two-microelectrode voltage clamp equipped with a bath-clamp circuit (OC-725B; Warner Instruments) as described before (Welling, 1997). In brief, oocytes were placed in a small Lucite chamber and incubated in either a 5 K [5 mM KCl, 85 mM *N*-methyl-d-glucamine (NMDG)–Cl, 1 mM $MgCl_2$, 1 mM $CaCl_2$, 5 mM HEPES, pH 7.4] or a 45 K (45 mM KCl, 45 mM NMDG-Cl, 1 mM $MgCl_2$, 1 mM $CaCl_2$, 5 mM HEPES, pH 7.4) artificial solution. When required, barium acetate was added to a concentration of 1 mM. Voltage-sensing and current-injecting electrodes had resistances of 0.5–1.5 MΩ when back filled with 3 M KCl. After a stable impalement was attained, such that both electrodes measured the same membrane potential, pulse protocols were conducted. Stimulation and data acquisition were performed with a Macintosh Centris 650 computer using an ITC16 analogue-to-digital, digital-to-analogue converter (Instrutech Corp.) and Pulse software (HEKA Electronik). Data were filtered at 1 kHz and digitized online at 2 kHz to the hard disk using Pulse and IGOR (WaveMetrics, Inc.) for later analysis.

Single channel properties were assessed 2–6 d after injection in the on-cell configuration with the patch-clamp technique (Hamill et al., 1981). In these studies, the vitelline membrane was removed from oocytes after hyperosmotic shrinking (Methfessel et al., 1986). All single channel recordings were performed under symmetrical $[K^+]$ conditions (150 mM KCl, 1 mM $CaCl_2$, 5 mM HEPES, pH 7.4). Patch-clamp electrodes, pulled from borosilicate glass (7052; Corning-Kovar Corp.), had resistances of 1–5 MΩ. Single channel currents were measured with an patch clamp amplifier (Axopatch 200A; Axon Instruments), digitized at a sampling rate of 47 kHz using a digital data recorder (VR-10B; Instrutech Corp.), and stored on a videotape. Data were acquired and analyzed using the Acquire and TAC family of programs (Bruxton Corp.). Data were replayed, filtered with an eight-pole Bessel filter (900; Frequency Devices Inc.) at a cut-off frequency of 1 kHz, and sampled at at least five times the filtering frequency. A 50% threshold criterion was used to detect events. Open and closed dwell-time histograms (logarithmic time scale, 10 bins/decade) were constructed from 15–60-s records and fit to exponential distributions using the maximum likelihood method (Sigworth and Sine, 1987). The single channel current magnitude was estimated by fitting Gaussian distributions to the current amplitude histograms or by measuring the amplitudes directly from analogue current traces. Inward slope conductance was assessed from such current measurements at −120 to −40 mV.

Data Analysis

Kir 1.1a and Kir 1.1a 331X coexpression experiments were analyzed using binomial probability theory, as first described for voltage-gated K^+ channels by Mackinnon (1991). Assuming mutant (mut) and wild-type subunits are coexpressed with equal efficiency and randomly assemble into a complex containing n subunits, binomial theory predicts that $(n + 1)$ different populations of channels will be formed with finite probabilities that are prescribed by the relative amounts of the two subunits [F^{mut} = nanograms mut cRNA/

(nanograms mut cRNA + nanograms wt cRNA)]. Two ideal cases were initially considered. For these models, it was also assumed that wild-type and mutant subunits oligomerize with equal efficiency and that any channel population is either fully active or fully inhibited. In the case of a complete dominant-negative effect in a tetrameric channel, the active channel population will be described by the probability of forming channels that are exclusively comprised of wild-type subunits, or $(1 - F^{mut})^4$. For a negative effect requiring two mutants within a tetramer, the active channel population will be described by the probability of forming channels that have less than two mutant subunits, or $(1 - F^{mut})^4 + 4\,F^{mut}\,(1 - F^{mut})^3$.

After considering these two possibilities, a modified probability equation, $I/I_o = (1 - kF^{mut})^4$, was developed to describe the Kir 1.1a 331X dominant negative effect. This model maintains the fundamental properties of a binomial distribution (i.e., random assembly of n subunits determined by F^{mut}), but accounts for deviations in mutant channel oligomerization efficiency or partial current inhibition by a single mutant subunit. Curve fitting for analysis of the dominant negative effect was performed using IGOR. The correction factor, k, was obtained by fitting normalized macroscopic current (I/I_o) as a function of F^{mut} with the modified probability equation, using a nonlinear, least squares, iterative algorithm (Levenberg-Marquardt).

Statistical evaluation of all data was performed with the GB-Stat™ v 5.0.6 for Macintosh statistics package (Dynamic Microsystems, Inc.). Where applicable, the pooled Student's t test was used to compare test groups. All data are given as mean ± SEM.

RESULTS

Deletion of the Last 60 Amino Acids of Kir 1.1a Abolishes Channel Activity

As a first approach to examine the functional consequences of COOH-terminal truncation, wild-type Kir 1.1a and Kir 1.1a 331X cRNAs were independently injected into *Xenopus* oocytes, and macroscopic currents were measured using two-microelectrode voltage clamp. As predicted from the link to Bartter's syndrome, truncation of the extreme COOH terminus of Kir 1.1a abolishes channel activity (Fig. 1). Oocytes injected with Kir 1.1a cRNA-expressed large, weakly inward rectifying macroscopic currents, typical of the wild-type channel (Ho et al., 1993). In contrast, no currents above the background could be detected in oocytes injected with Kir 1.1a 331X cRNA. The mean Ba^{2+}-sensitive macroscopic current at −90 mV was −0.11 ± 0.05 μA (n = 6), compared with −17.95 ± 2.87 μA (n = 12) for the wild-type channel. Consistent with the macroscopic data, no significant activity, except for occasional endogenous stretch-activated channel openings (Yang and Sachs, 1990), was detected in oocytes injected with the mutant cRNA (see Fig. 6 C, n = 12).

To determine the function of the Kir 1.1a COOH-terminal domain, we elucidated the mechanism causing the defect in this particular Bartter's mutant. Obviously, the magnitude of macroscopic Kir 1.1a current is a product of the number of channels in the membrane, the open probability of the channel, and the single channel conductance. Truncation of the extreme COOH-terminal 60 amino acids of Kir 1.1a can abolish channel activity by reducing any of these quantities, alone or in combination. The number of channels in the membrane may be reduced by a global structural

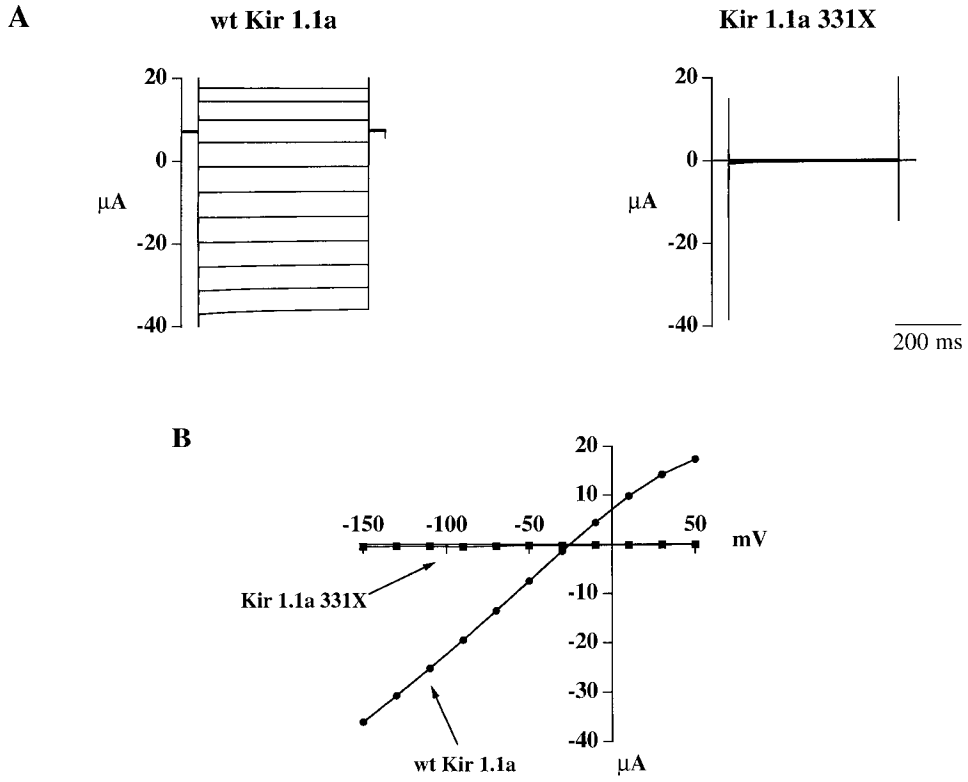

Figure 1. Truncation of amino acids 332–391 (Kir 1.1a 331X) disrupts Kir 1.1a channel functional expression. (A) Representative families of whole-cell currents and (B) macroscopic current-voltage relationships measured from *Xenopus* oocytes injected with either Kir 1.1a (●) or Kir 1.1a 331X (■) cRNA (250 pg) using two-microelectrode voltage clamp. Currents were elicited by 500-ms voltage clamp pulses from −150 to +50 mV in 20-mV increments (V_{HOLD} = 0 mV; $[K^+]_o$ = 45 mM). This pulse protocol was used in all subsequent measurements of macroscopic channel activity, unless otherwise noted.

alteration, loss of an essential oligomerization domain, or a defect in membrane trafficking or plasma membrane stability. Alternatively, the mutant channels may be expressed in the plasma membrane in a nonconductive or nonfunctional conformation. The potential mechanisms underlying the Kir 1.1a 331X defect implicate different functional roles for the extreme COOH-terminal domain, therefore we explored each.

Mutant Channels Can Oligomerize with Wild-Type Subunits

An oligomerization defect or global structural mutation can be easily tested by coexpressing the mutant with the wild-type channel. If the mutant protein is synthesized, folded correctly, and capable of oligomerization, the macroscopic current in oocytes coinjected with wild-type and mutant cRNA is predicted to be less than oocytes injected with wild-type alone. Fig. 2 B summarizes the results of such a study. Coexpression of Kir 1.1a 331X with the wild-type channel reduced Ba^{2+}-sensitive macroscopic current by 62 ± 5%, demonstrating that the mutant is capable of exerting a negative influence on the wild-type channel (n = 12, Kir 1.1a 331X; n = 18, Kir 1.1a; $P < 0.005$).

To ensure that the Kir 1.1a 331X effect is specific and not due to the competition of mutant cRNA for the translational machinery, the experiment was repeated with an unrelated dominant negative Kir channel, Kir 3.1-AAA. Kir 3.1 was made nonconductive by replacing the key Gly-Tyr-Gly K^+-selectivity sequence (amino acids 145–147) with three Ala residues (Tinker et al., 1996). Kir 3.1, a G protein–gated Kir channel, is not thought to oligomerize with Kir 1.1a. As shown in Fig. 2 B, Kir 3.1-AAA exhibited no influence on Kir 1.1a expression. This result indicates that the translation of Kir 1.1a cRNA is not inhibited when a second transcript is coinjected. Instead, the dominant negative effect of Kir 1.1a 331X is due to the oligomerization of mutant and wild-type subunits.

To gain further insight into the dominant negative mechanism, increasing doses of mutant cRNA were coinjected with a constant amount of wild-type transcript (Fig. 3; n = 5–14 each dose). Because Kir 1.1a channels are known to be tetrameric in structure (Glowatzki et al., 1995), coinjection should produce five discrete populations, containing zero to four mutant subunits. Assuming random assembly, a binomial probability distribution defined by two parameters, F^{mut} and n, determines the probability of obtaining each channel population. F^{mut}, the mutant fraction of the total cRNA injected [F^{mut} = nanograms mut cRNA/(nanograms mut cRNA + nanograms wt cRNA)], is the probability of incorporating a Kir 1.1a 331X subunit. For a tetrameric channel, the number of subunits, n, is equal to 4. The relative frequency of functional populations determines the resultant macroscopic current density. The pre-

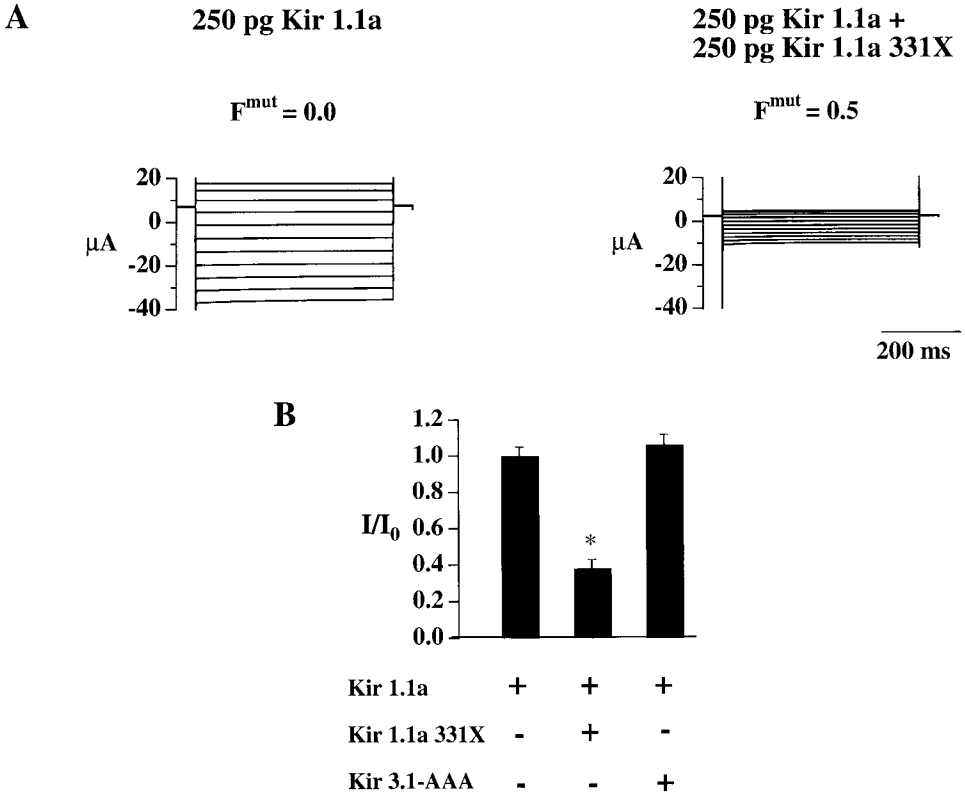

Figure 2. Deletion of the extreme COOH terminus does not cause a global structural mutation or prevent subunit oligomerization. (A) Representative families of whole cell currents recorded from oocytes injected with either Kir 1.1a (250 pg) or Kir 1.1a and Kir 1.1a 331X (250 pg each) cRNA. (B) Ba^{2+}-sensitive macroscopic currents (V_m = −90 mV) measured in oocytes coinjected with equivalent amounts of cRNA encoding Kir 1.1a and Kir 1.1 331X or Kir 1.1a and Kir 3.1-AAA (250 pg each), normalized to the mean current of the control group injected with Kir 1.1a alone (250 pg) (*$P <$ 0.005). Kir 3.1-AAA is a mutant, nonconductive form of a G protein–gated Kir channel that exerts a dominant negative effect on Kir 3.1, but does not oligomerize with Kir 1.1a.

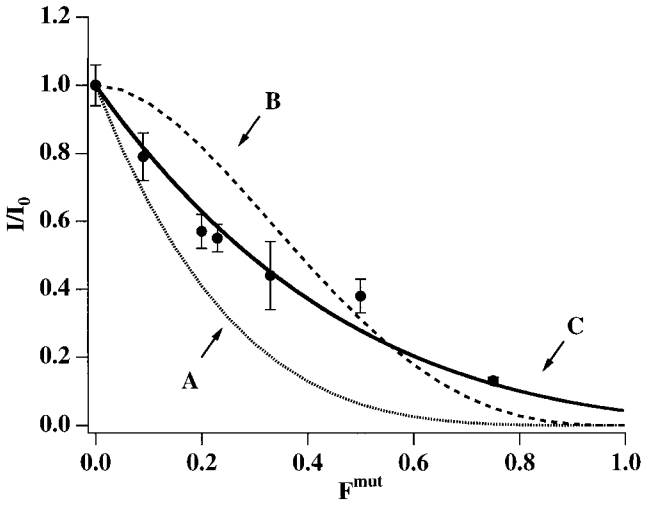

Figure 3. Dominant negative effects of Kir 1.1a 331X on wild-type Kir 1.1a. Ba^{2+}-sensitive inward current is plotted (I/I_o, V_m = −90 mV) as a function of F^{mut}, the mutant fraction of the total cRNA injected [F^{mut} = nanograms mut cRNA/(nanograms mut cRNA + nanograms wt cRNA)]. F^{mut} was adjusted by coinjecting variable amounts of Kir 1.1a 331X with a constant dose of Kir 1.1a (250 pg), and I_o is the mean current when $F^{mut} = 0$. The dotted line (A) represents the predicted relationship if inclusion of one or more mutant subunits within a tetramer inhibits channel function [$I/I_o = (1\ F^{mut})^4$]. The dashed curve (B) is predicted if two or more subunits are required [$I/I_o = (1 - F^{mut})^4 + 4(1 - F^{mut})^3F^{mut}$]. The data are best fit by an intermediate model, $I/I_o = (1 - 0.6\ F^{mut})^4$, represented by the solid line (C). The coefficient, *k*, is less than unity, indicating that a single mutant subunit partially inhibits current or that Kir 1.1a331X oligomerizes with a reduced efficiency.

dicted relationships for two specific dominant negative models are shown in Fig. 3. Consider the situation when incorporation of one or more mutant subunits abolishes channel activity. The relative current is determined by the probability of assembling four wild-type subunits into a tetramer. In this case, the macroscopic current can be predicted by the relationship, $I/I_o = (1 - F^{mut})^4$ (Fig. 3, line A). If two or more mutants must be incorporated within a tetramer to inhibit channel activity, an additional term, the probability of forming a channel with one mutant and three wild-type subunits [$4\ F^{mut}(1 - F^{mut})^3$], is added to the equation above (line B).

As shown in Fig. 3, neither ideal model could adequately describe the Kir 1.1a 331X dominant negative effect. Instead, to characterize this particular dominant negative mutant, the data was fit to a modified probability equation, $I/I_o = (1 - kF^{mut})^4$, where the coefficient, *k*, is a correction factor that can take into account variations in oligomerization efficiency or partial current inhibition. The intermediate model (line C) required a *k* factor of 0.6 to accurately describe the data, suggesting that Kir 1.1a 331X has a reduced oligomerization efficiency (~60% compared with wild type) or that a single mutant subunit only partially inhibits channel activity. In the former case, the probability of incorporating a mutant is lower than predicted from the ratio of cRNA injected. In the latter instance, the measured I/I_o reflects not only the wild-type population, but also the relative frequency of channels that contain a mutant and carry a diminished current. Because the two possibilities have different implications for the function of the extreme COOH-terminal domain, the source of the intermediate model was resolved by the experiment described below.

Intermediate Dominant Negative Model Is Due to a Reduced Oligomerization Efficiency

To critically test the effects of incorporation of a single mutant into a Kir 1.1a channel and determine the origin of the intermediate model, three different tetrameric concatemer cDNAs (4wt, 3wt + 1mut, and 1mut + 3wt) were engineered. By creating tandem concatemers, the functional consequences of incorporating a single mutant subunit within a tetrameric channel can be assessed in a manner that is independent of oligomerization efficiency. As described in methods, four monomeric Kir 1.1a cDNAs were artificially linked together with codons for 10 glutamine residues. Glutamine linkers have been successfully used in previous studies to link potassium channel subunits together (Yang et al., 1995b) and are thought to possess little secondary structure and exert minimal influence on channel function. As shown in Fig. 4, we validated this approach by examining the functional characteristics of 4wt and the effects of Kir 1.1a 331X monomers on concatenated channels.

To confirm that covalent linkage of subunits does not perturb channel structure or function, we compared the biophysical properties of wild-type and concatenated Kir 1.1a. Injection of the 4wt tandem tetramer cRNA ($n = 22$) into oocytes produced K^+ channels that exhibited weak inward rectification and voltage-dependent block by extracellular Ba^{2+} (not shown) identical to wild-type Kir 1.1a ($n = 12$, Fig. 4 B). Moreover, covalent linkage of wild-type subunits had no effect on single channel properties ($n = 7$ each). These results are summarized in Fig. 4, D and E. Both wild-type Kir 1.1a and the 4wt concatemer had identical open probability (0.93 ± 0.01 vs. 0.94 ± 0.004, respectively) and single channel conductance (37 ± 2.47 vs. 39.6 ± 1.26 pS, respectively). Like the wild-type channel, the kinetics of the concatemer are best described by single open (Kir 1.1a, $\tau_o = 20 \pm 0.87$ ms; 4wt, $\tau_o = 18 \pm 1$ ms) and closed times (Kir 1.1a, $\tau_c = 1.1 \pm 0.03$ ms; 4wt, $\tau_c = 1.05 \pm 0.04$ ms). These data clearly demonstrate that the tandem tetramer precisely recapitulates wild-type channel function.

To ensure that the four concatenated subunits contribute to channel formation, the 4wt concatemer was coexpressed with either the dominant negative Kir 1.1a

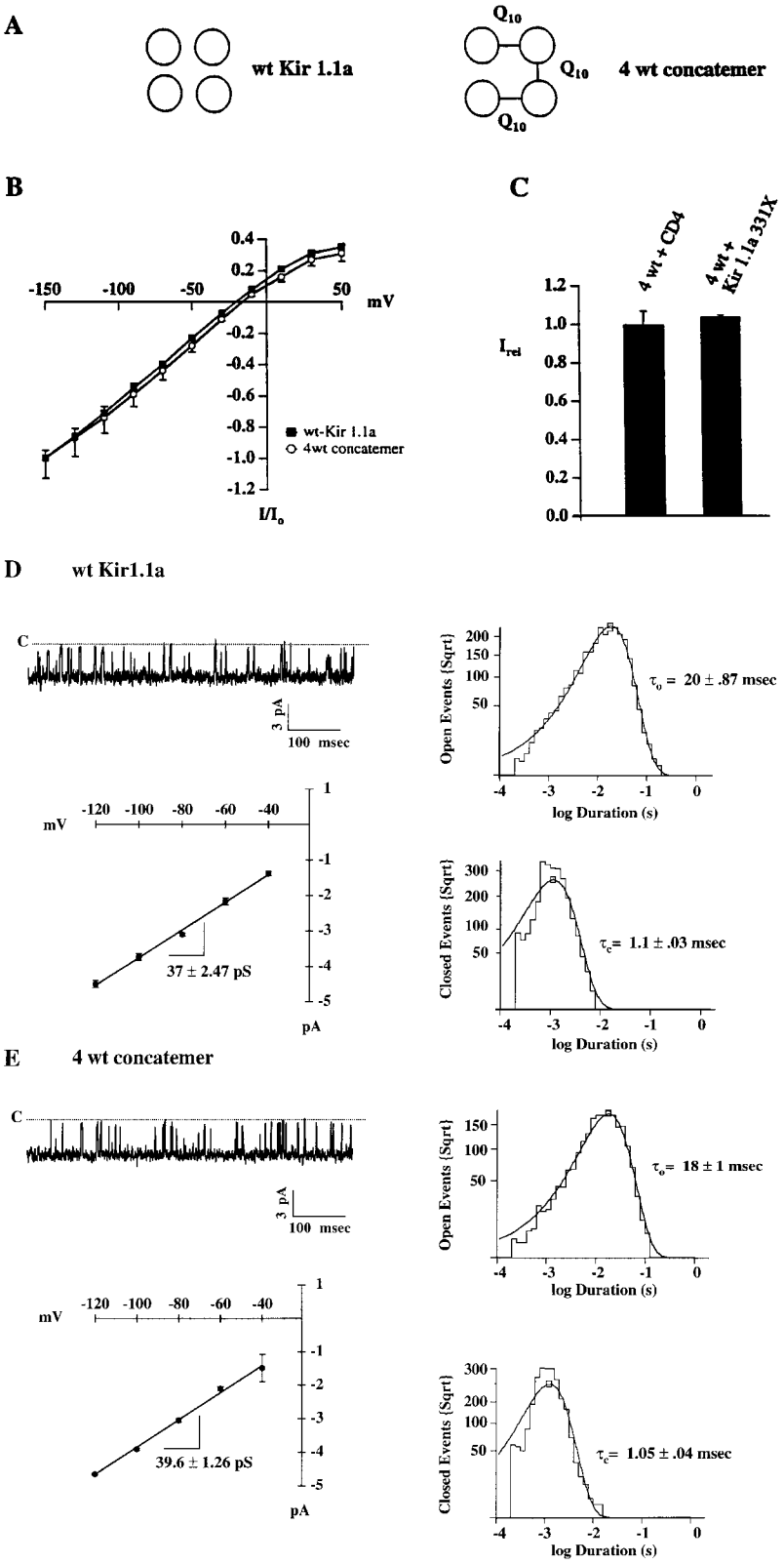

Figure 4. Tandem covalent linkage of four wild-type Kir 1.1a subunits constrains channel stoichiometry without altering the biophysical properties. (A) Wild-type Kir 1.1a channels were expressed either as monomers (wt Kir 1.1a) or concatemers (4wt) where four subunits were covalently linked in a head-to-tail fashion via a 10 glutamine residue linker (see text for details). (B) Oocytes injected with cRNA encoding either wt Kir 1.1a (■) or the 4wt concatemer (□) exhibited weakly inward rectifying macroscopic currents that were blocked in a voltage-dependent manner by Ba^{2+} (not shown). Shown are currents, normalized to the mean amplitude at −150 mV (I/I_o), as a function of voltage. (C) There is no dominant negative effect of Kir 1.1a 331X monomers on concatemeric tetramers, confirming that 4wt channels are comprised of a single tetrameric protein. Shown are currents (V_m = −90 mV) measured in oocytes coinjected with the 4wt concatemer and Kir 1.1a 331X normalized to the mean current in the control group that was coinjected with the 4wt concatemer and an unrelated cRNA, CD4. Representative single channel cell-attached recordings obtained from oocytes injected with either (D) wild-type Kir 1.1a or (E) 4wt concatemer cRNA (top left, V_m = −80 mV). Inward currents are examined so upward deflections represent channel closures. The current–voltage relationship (bottom left), open (top right), and closed (bottom right) dwell-time histograms are shown for each. The single channel conductance of the wild-type and concatemeric channel are identical. The solid line in each dwell-time histogram represents the log-likelihood fit to the experimental data. The kinetics of both channels were best described by single open and closed times, although in some patches a longer lived (τ = 20 ms) closed state, as described by Choe et al. (1998), accounted for <0.5% of channel closures. Both the wild-type and concatemeric channels exhibited a high open probability (0.93 ± 0.01 vs. 0.94 ± 0.004, respectively).

331X or an unrelated gene product, CD4. The results of these studies are summarized in Fig. 4 C. As predicted if the four concatenated subunits form functional channels, 4wt concatemer currents were not affected by coexpression of the dominant negative mutant, Kir 1.1a 331X (n = 11). These observations confirm that channels are indeed formed from a single protein rather than portions of multiple concatemers.

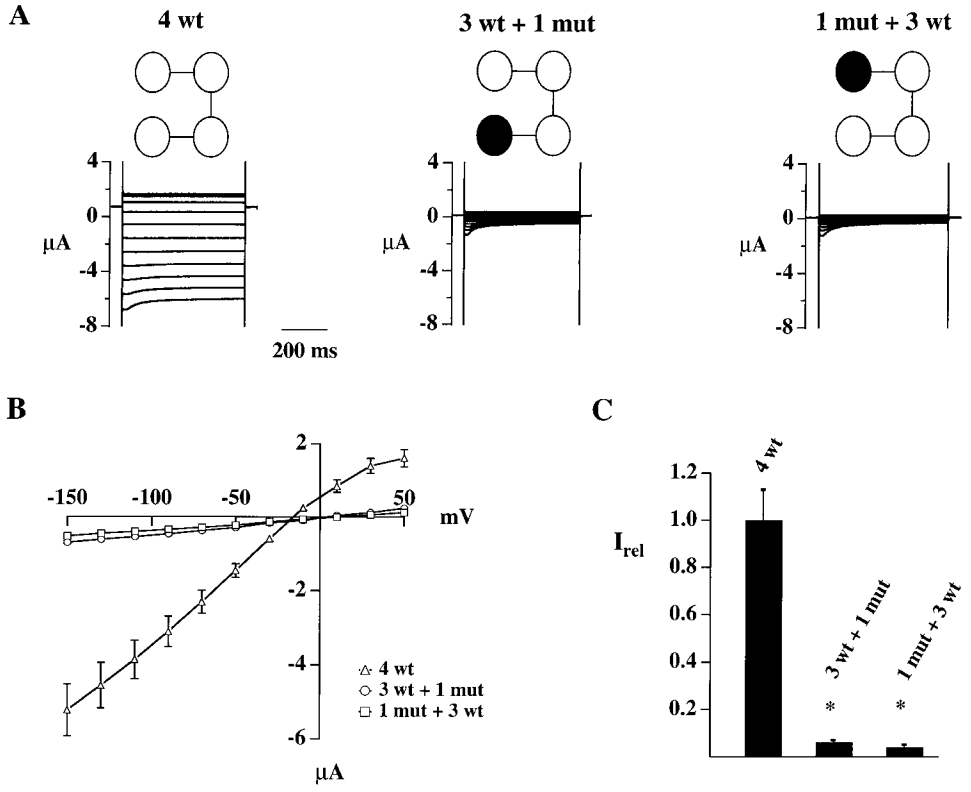

Figure 5. Incorporation of single Kir 1.1a 331X mutant at either the NH_2- or COOH-terminal position of a tandem tetramer suppresses channel activity. (A) Representative families of whole-cell currents, (B) composite current–voltage relationships, and (C) normalized macroscopic Ba^{2+}-sensitive currents ($V_m = -90$ mV) measured from oocytes injected with equivalent amounts of 4wt, 3wt + 1mut, or 1mut + 3wt concatenated tetramer cRNA (1 ng; $*P < 0.0001$) are shown.

Having demonstrated that concatenation of subunits does not affect channel function, we tested the functional effects of Kir 1.1a 331X within a tandem tetramer. Incorporation of a single mutant within the concatemeric tetramer, at either the NH_2- or COOH-terminal positions (1mut + 3wt or 3wt + 1mut, respectively) completely suppressed macroscopic channel activity. These results are summarized in Fig. 5. In contrast to the 4wt concatemer (-2.56 ± 0.34 μA, $n = 25$), the 1mut + 3wt and 3wt + 1mut concatemers exhibited no measurable currents above background (-0.15 ± 0.03 and -0.10 ± 0.02 μA, respectively, $n = 12$, $P < 0.0001$). The complete dominant negative effect was confirmed at the single channel level. Except for occasional endogenous stretch-activated channel openings in some patches, no significant activity could be detected in on-cell patches of oocytes injected with either mutant-containing concatemer (Fig. 6, 3wt + 1mut, $n = 14$, total recording time = 56 min; 1mut + 3wt, $n = 17$, total recording time = 31 min).

Because Kir 1.1a 331X exerts a complete dominant negative effect when constrained by the covalent linkage of a concatenated tetramer, it is clear that the intermediate dominant negative model results from an ~40% reduction in oligomerization efficiency. The role of the extreme COOH terminus in governing the efficiency of subunit assembly is consistent with both the recessive nature of Bartter's disease and two previous reports that implicated the COOH terminus in tetramerization (Tinker et al., 1996; Koster et al., 1998). While this domain influences Kir 1.1a oligomerization efficiency, these results collectively demonstrate that COOH-terminal truncation has more important functional consequences downstream of channel assembly.

Both Kir 1.1a and Kir 1.1a 331X Are Expressed on the Oocyte Plasma Membrane

To test the role of the COOH-terminal domain (amino acids 332–391) in determining membrane trafficking and plasma membrane stability, NH_2-terminal enhanced green fluorescent protein fusion proteins of Kir 1.1a and Kir 1.1a 331X were constructed and expressed in oocytes. This strategy was favored over an antibody binding assay (Firsov et al., 1996) because incorporation of an external epitope (Flag or AUI) abolished Kir 1.1a function. As shown in Fig. 7, NH_2-terminal attachment of EGFP had no effect on the single channel conductance ($\gamma = 39 \pm 3$ pS) or high open probability kinetics of ($P_o = 0.91 \pm 0.01$) of Kir 1.1a ($n = 4$). The lack of EGFP-dependent functional effects offers compelling evidence that channel structure is not altered by the NH_2-terminal fusion protein.

As shown in Fig. 8, whole, unfixed oocytes injected with EGFP fusion protein cRNA were examined using laser scanning confocal microscopy. Uninjected oocytes exhibited a low basal autofluorescence. EGFP was widely distributed throughout the cytoplasm ($n = 6$).

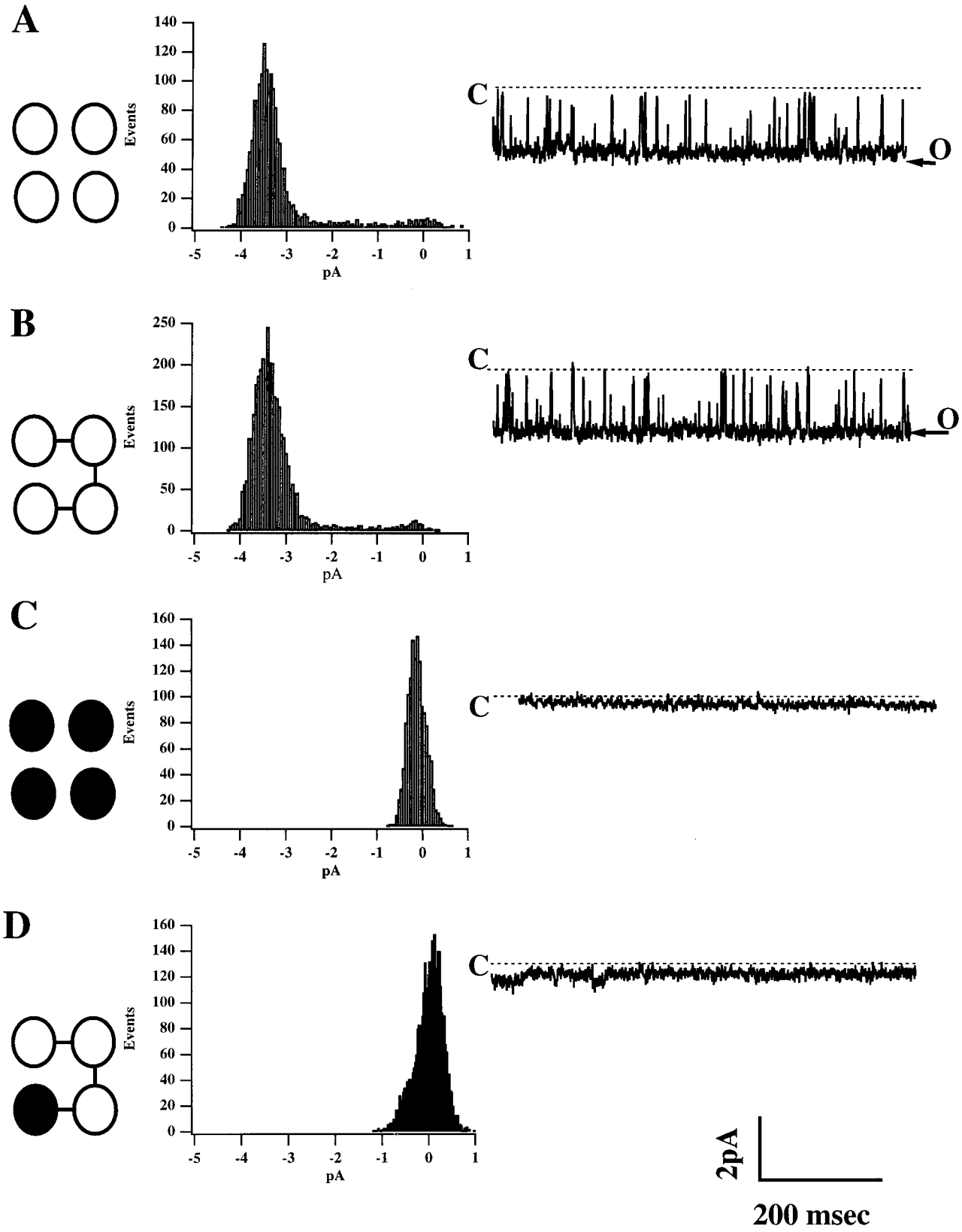

Figure 6. The complete dominant negative effect of one Kir 1.1a 331X is confirmed in single channel recordings. Single channel records and corresponding all-points amplitude histograms were obtained in cell-attached mode at $V_m = -80$ mV from oocytes injected with either (A) wt Kir 1.1a, (B) 4wt concatenated tetramer, (C) Kir 1.1a 331X, or (D) 3wt + 1mut concatenated tetramer. Occasional small-conductance channel events could be detected in some recordings from oocytes injected with the mutant or mutant-containing concatemer cRNA. These do not likely reflect mutant channel function, as similar events could be detected in uninjected oocytes. Identical results were obtained for both mutant-containing concatemers (1mut + 3wt, not shown).

In contrast, both EGFP-Kir 1.1a and EGFP-Kir 1.1a 331X were localized along a distinct zone circumscribing the oocyte (n = 6 in each injection dose). The circumferential fluorescence pattern was maintained in sequential z-plane optical sections through the entire oocyte, consistent with predominant plasma membrane expression. Fluorescence intensity was proportional to the amount of fusion protein cRNA injected, and no significant difference could be detected between EGFP-Kir 1.1a and EGFP-Kir 1.1a 331X at any injection dose (Fig. 8 B). These data support the premise that both channels are expressed on the plasma membrane with equal efficiency.

Comparison of macroscopic conductance with plasma membrane delimited fluorescence intensity in oocytes injected with either EGFP fusion protein (n = 5) further strengthens this conclusion. The results of these studies are summarized in Fig. 8 C. The macroscopic conductance was directly proportional to fluorescence intensity in oocytes injected with EGFP-Kir 1.1a, as predicted if circumferential fluorescence intensity is proportional to the number of channels in the plasmalemma. Consequently, the observation that the circumferential fluorescence distribution and intensity of the Kir 1.1a 331X mutant is indistinguishable from the wild-type channel provides evidence that the mutant channel is also primarily expressed on the plasma membrane.

Collectively, these results suggest that the entire extreme COOH terminus of Kir 1.1a (amino acids 332–391) is not necessary to direct Kir 1.1a plasma membrane targeting and stability in the *Xenopus* oocyte expression system. Subsequently, loss of function in the Bartter's mutant, Kir 1.1a 331X, is not due to a reduction of the number of channels in the plasmalemma. Instead, mutant channels exist in a nonconductive or inactive conformation. This conclusion was confirmed by examining a series of COOH-terminal truncated mutants as described below.

Gating Defect Revealed in the Minimal Functional Channel, Kir 1.1a 351X

Having found that the extreme COOH terminus is involved in maintaining channel activity, we delimited the minimal domain that is required for functional expression in the hopes of revealing the mechanism underlying the Kir 1.1a 331X defect. In these studies, the channel was gradually reconstructed by sequentially adding

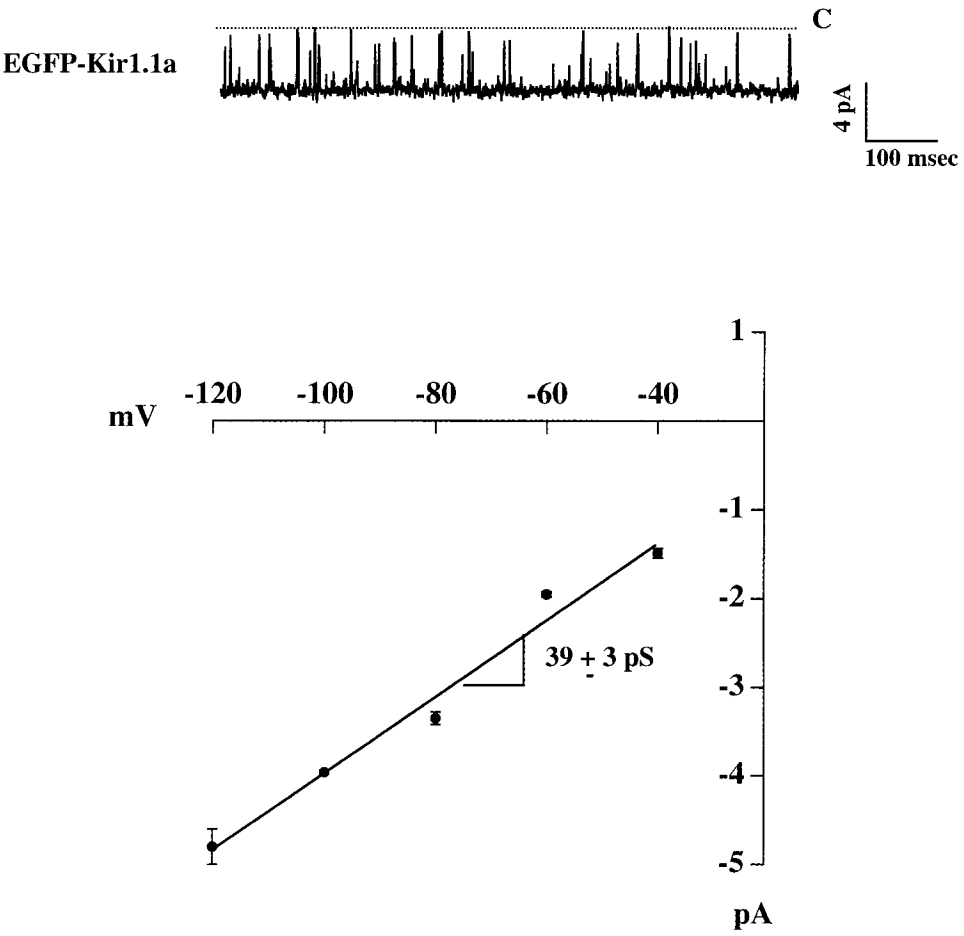

Figure 7. Fusion of EGFP to the Kir 1.1a NH_2 terminus does not alter channel function. Shown are representative single channel recording (V_m = −80 mV) and corresponding current–voltage relationship, obtained in the cell-attached mode from oocytes injected with EGFP-Kir 1.1a cRNA. EGFP-Kir 1.1a opens with the identical inward slope conductance (bottom) and open probability (0.91 ± 0.01) as the wild-type channel.

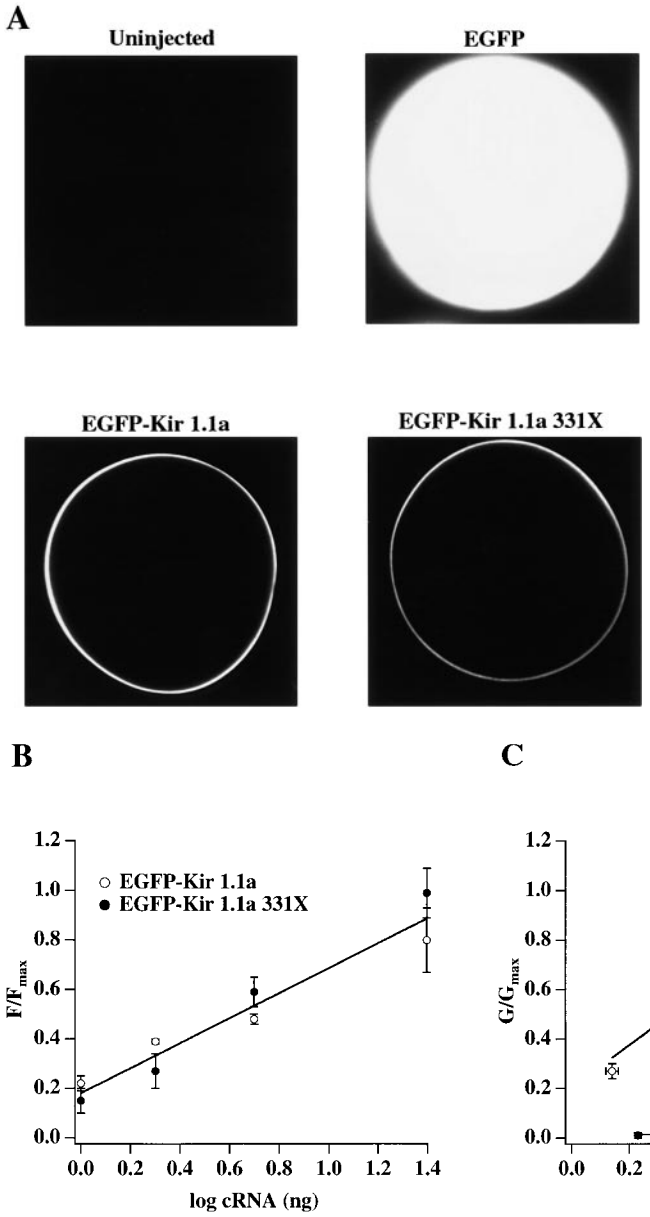

Figure 8. COOH-terminal truncation does not alter Kir 1.1a trafficking or plasma membrane stability in the *Xenopus* oocyte expression system. (A) Representative optical sections acquired from oocytes at a focal plane near the equator using laser-scanning confocal microscopy. Oocytes injected with EGFP, EGFP-Kir 1.1a, or EGFP-Kir 1.1a 331X cRNA were compared with uninjected oocytes. (B) Circumferential fluorescence intensity plotted as a function of the fusion protein cRNA dose injected. No significant differences in circumferential fluorescence distribution and intensity were detected at any injection dose. The solid line represents the linear regression fit of the average circumferential fluorescence for oocytes injected with either wild-type or mutant fusion protein cRNA. C) Macroscopic conductance was measured in oocytes injected with either fusion construct at several cRNA injection doses and is plotted as a function of plasma membrane delimited fluorescence. Slope conductance was determined between −110 and −30 mV from oocytes bathed in 5 mM $[K^+]_o$. No conductance above background was detected in oocytes expressing EGFP-Kir 1.1a 331X, consistent with the premise that Kir 1.1a 331X resides in the plasma membrane but is in a nonconductive or inactive conformation.

portions of the extreme COOH terminus back to Kir 1.1a 331X (Fig. 9 A). Addition of amino acids 332–351 was sufficient to rescue minimal channel function, while deletion of this domain in isolation (Kir 1.1a Δ332–351) resulted in the loss of channel function. The results of these studies are summarized in Fig. 9 B. Oocytes injected with either Kir 1.1a 341X or Kir 1.1a Δ332–351, like Kir 1.1a 331X, exhibited no Ba^{2+}-sensitive currents above background (n = 6–11). In contrast, Kir 1.1a 351X–injected oocytes displayed significant weakly inward-rectifying, Ba^{2+}-sensitive macroscopic currents (n = 10, $P < 0.001$). Current density increased further with the addition of 10 more residues (Kir 1.1a 361X, n = 11, $P < 0.0001$). The addition of five more residues (Kir 1.1a 366X, n = 10) failed to produce a further significant increase in channel activity. Collectively, these studies define amino acids 332–351 as the critical COOH-terminal domain within the extreme COOH terminus that is absolutely required for maintaining channel activity.

By identifying an active channel retaining a defect, Kir 1.1a 351X, the mechanism underlying the role of the COOH-terminal domain could be uncovered. The nature of the defect was elucidated by comparing the single channel properties (cell-attached configuration) of Kir 1.1a 351X (n = 5) to the wild type (n = 4). Aberrant gating behavior was revealed in long duration (∼20 min) recordings, where P_o was continuously mon-

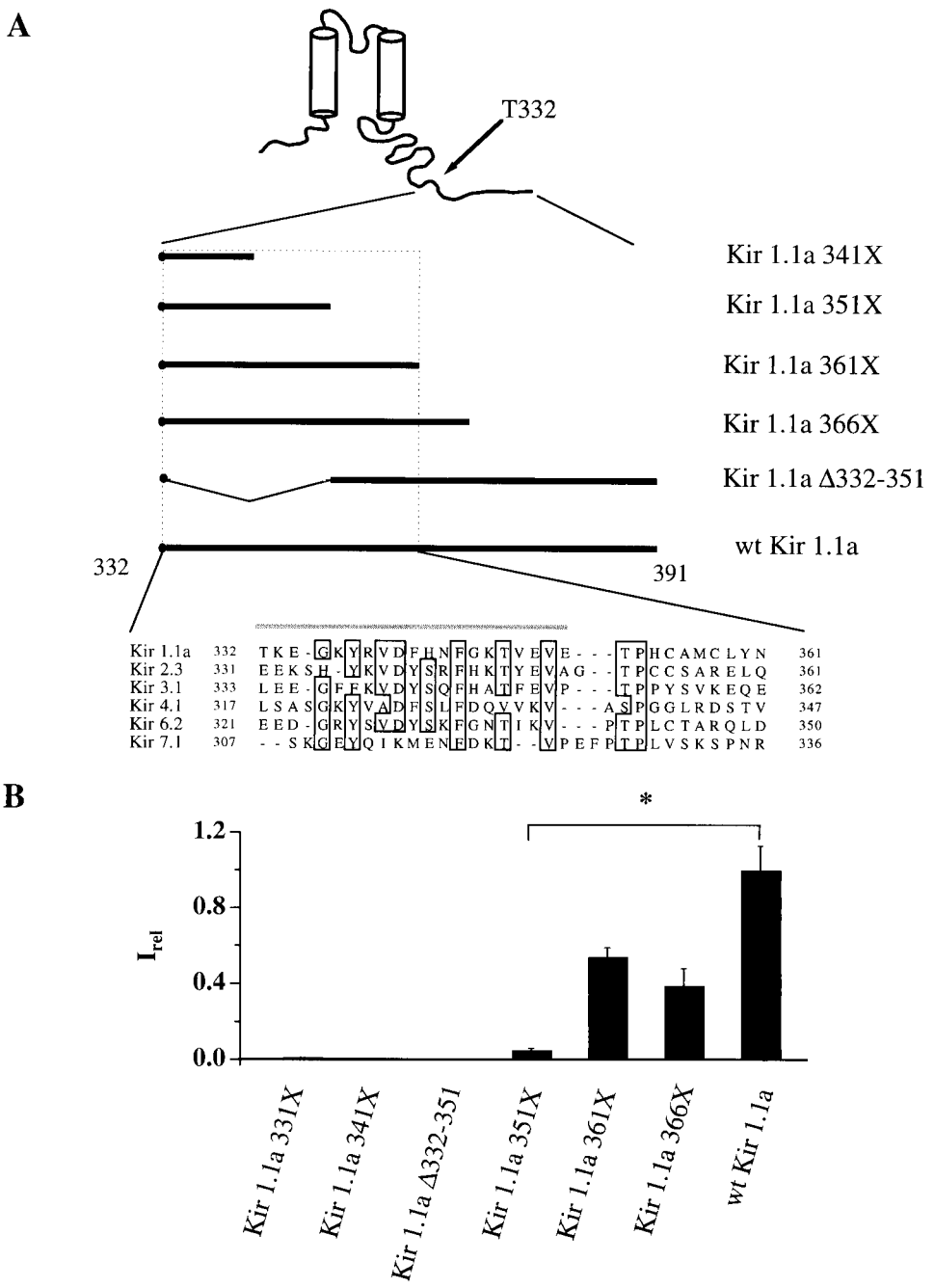

Figure 9. A series of truncated mutants delimit amino acids 332–351 as the COOH-terminal domain necessary to maintain channel function. (A) Kir 1.1a channels were reconstructed by adding residues back to the Bartter's mutant, Kir 1.1a 331X. Amino acids 332–361 represent the most conserved domain (30% identity) within the extreme COOH terminus of inward rectifying K^+ channels. (B) Shown are normalized Ba^{2+}-sensitive whole cell currents (V_m = −90 mV) obtained from oocytes expressing each of the truncated mutants depicted in A (*P < 0.01). Replacement of amino acids 332–351 (Kir 1.1a 351X) restored channel activity, while deletion of this domain (Kir 1.1a Δ332-351) abolished macroscopic currents.

itored in 15-s intervals. The results from two representative recordings are shown in Fig. 10 A. In contrast to the sustained high open probability kinetics of the wild-type channel, Kir 1.1a 351X channels exhibited bursts of channel activity, "active gating," interrupted by sojourns in a long-lived inactive mode ($t_{inactive}$ = 5.12 min). As a consequence of the long-lived inactive state, the open probability of the Kir 1.1a 351X was significantly reduced compared with the wild-type channel (0.36 ± 0.02 vs. 0.91 ± 0.01, respectively; $P < 0.0001$). During the active gating mode, Kir 1.1a 351X channels exhibited the same single channel conductance (γ = 40 ± 2 pS), open and closed times (τ_o = 20 ± 1.2 ms; τ_c = 1.2 ± 0.1 ms) as wild-type channels (Fig. 11), indicating that the COOH-terminal deletion does not alter the conduction pathway. Truncating the extreme COOH terminus of Kir 1.1a reduces channel activity by dramatically increasing the probability of exhibiting an inactive gating mode. This phenotype is unique to Kir 1.1a 351X; the open probability and single channel

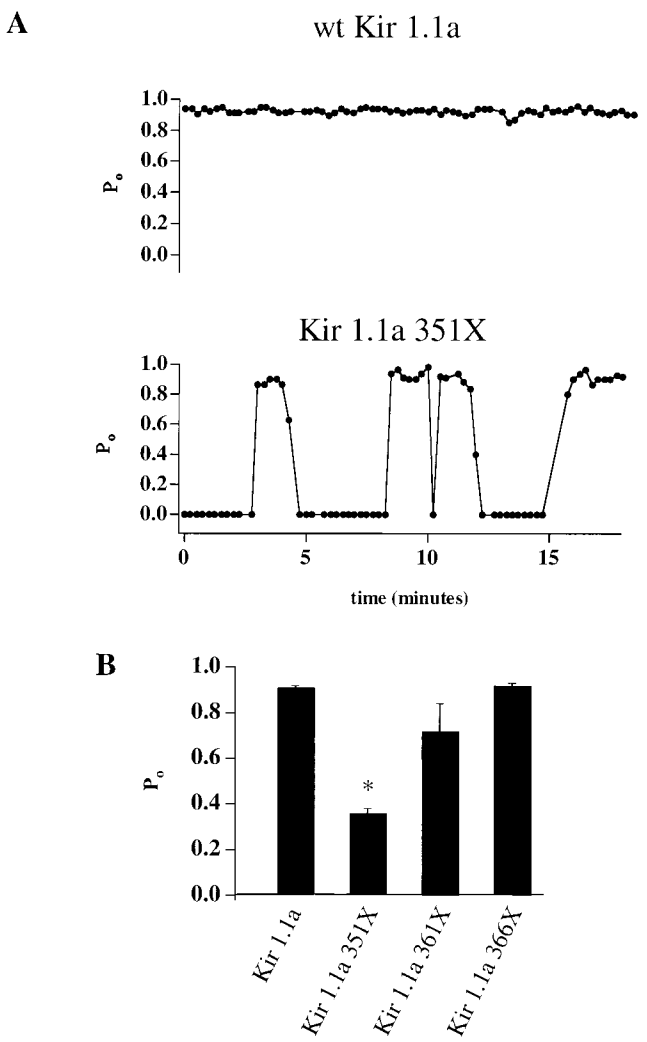

Figure 10. COOH-terminal truncation stabilizes an aberrant inactive gating mode. (A) Diary plots of single channel activity in Kir 1.1a 351X vs. the wild type. Shown are plots of open probability measured in 15-s intervals over 20 min. Single channel recordings were obtained in the cell-attached mode ($V_m = -80$ mV) from oocytes injected with either wild-type or Kir 1.1a 351X cRNA. The mutant exhibits an inactive mode that has a mean lifetime of 5.12 min. (B) Average open probabilities for both wild-type and truncated mutants (n = 4–5) measured over the duration of a 15–20-min recording (*$P < 0.0001$). The reduced P_o of Kir 1.1a 351X results from the stabilization of the long-lived inactive state.

conductance of Kir 1.1a 361X and Kir 1.1a 366X are not statistically different from the wild-type channel (Fig. 10 B).

Although Kir 1.1a 361X and Kir 1.1a 366X gating kinetics were unchanged from the wild type, the macroscopic current amplitude of the wild-type channel was significantly greater than these COOH-terminal deletion mutants. This may reflect a defect in channel trafficking or stability in the plasma membrane, or a significant silent channel population. Nevertheless, these studies define amino acids 332–351 as the domain within the extreme COOH terminus that is absolutely required for maintaining Kir 1.1a channels in the open state.

DISCUSSION

The identification of disease-causing mutations in the Kir1.1a channel provides insightful clues about important functional domains that have previously escaped attention. For instance, a particular Bartter's-linked mutation, a frame shift (T332–K333) that replaces the last 60 carboxyl-terminal amino acids (332–391) with an entirely different 34-residue domain (Simon et al., 1996b), implicated the extreme COOH terminus as an obligate functional element. As predicted by this hypothesis, truncation of the COOH-terminal domain (Kir 1.1a 331X) produced a complete loss-of-function phenotype. By elucidating the mechanism underlying the defect in Kir 1.1a 331X, we discovered that the extreme COOH terminus acts as an obligate determinant of channel gating, maintaining the channel in a stable open state.

This conclusion is supported by several lines of evidence. Because Kir 1.1a 331X is efficiently expressed on the plasma membrane, loss-of-function must be a consequence of an inactive conformation rather than defective surface expression. By characterizing a series of progressively smaller truncations, a minimal COOH-terminal domain that is sufficient to rescue function was defined (332–351), and a discrete gating defect was uncovered. Mutant channels that are truncated at the extreme boundary of the required domain (351X) display marked inactivation behavior characterized by frequent occupancy in a long-lived closed state. Upon spontaneous recovery from inactivation, 351X acquired an active-gating mode that exhibits precisely the same conductance and kinetic properties as the wild-type channel. Because these biophysical attributes reflect the unique signature of K^+ permeation through the Kir 1.1 pore (Lu and Mackinnon, 1994; Choe et al., 1998), the mutational effect of 331X must result from aberrant gating rather than a permanent or profound distortion of the conduction pathway. Collectively, these data demonstrate that the extreme COOH-terminal domain is required to maintain channels in the open state; channels lacking this modulatory structure appear to be locked in a closed conformation.

It should be pointed out that our result with the 331X mutant in oocytes differs from a recent report of Schwalbe et al. (1998), who investigated the natural T332-K333 frameshift mutation in Sf9 insect cells. These investigators reported that channels bearing the T332 frameshift mutation are predominantly localized in an intracellular compartment of Sf9 cells, presumably the Golgi. This may reflect that the plasma membrane expression of the Kir 1.1 channel is dependent on the host cell type (Brejon et al., 1999). Alternatively,

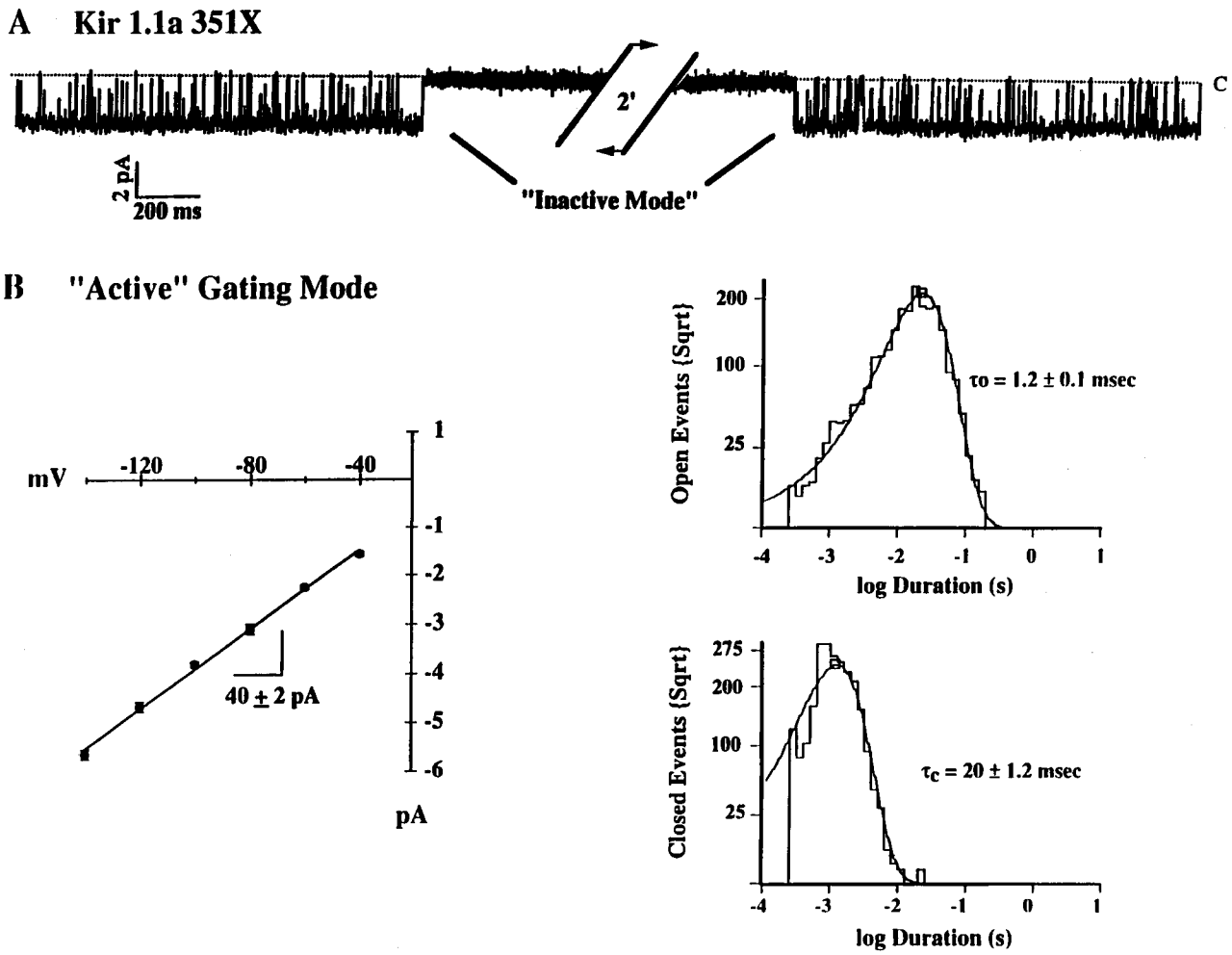

Figure 11. Upon spontaneous recovery from inactivation, Kir 1.1a 351X channels exhibit wild-type biophysical properties. (A) A typical single channel record (cell attached mode, $V_m = -80$ mV) illustrating the transition from active to inactive gating conformations. (B) The single channel conductance (left) and mean open (bottom right) and closed (top right) lifetime histograms of Kir 1.1a 351X in the active gating mode are indistinguishable from the wild-type channel (compare with Fig. 4).

the entirely different 34-residue domain that is introduced by the frameshift mutation may prevent proper trafficking to the cell membrane. While we cannot rule out a role for this domain in channel trafficking, we found in *Xenopus* oocytes where the channel is efficiently expressed that the COOH-terminal domain normally acts as an essential regulator of gating.

Presently, we cannot state with any certainty how partial truncation of the COOH terminus alters channel structure and how this favors the occupancy of a quiescent state; however, several mechanisms can be considered. For instance, the mechanism by which intracellular pH (Fakler et al., 1996; Choe et al., 1997; McNicholas et al., 1998) and PKA (McNicholas et al., 1994) regulate Kir1.1a activity provides some insight into the modulatory role of the carboxyl terminal domain. Kir1.1 activity is dependent on PKA-mediated phosphorylation of three serine residues (S44, S219, S323) located within the NH_2- and COOH-terminal domains (Xu et al., 1996; MacGregor et al., 1998), whereas a drop in cytoplasmic pH, sensed at K80 (Fakler et al., 1996; Choe et al., 1997), inhibits the channel. Because dephosphorylation (MacGregor et al., 1998) and cytoplasmic acidification (Choe et al., 1997) induce a state that resembles the gating conformation conferred by the 351X mutation, it is tempting to speculate a common or coupled gating pathway. In this view, the extreme carboxyl terminal domain may directly influence physiologic regulation of the channel in one of two different ways. The domain could directly interact with the phosphoacceptor and pH-sensing sites, similar to the way the NH_2-terminal domain in cyclic nucleotide–gated channels interacts with the cyclic nucleotide–binding domain (Varnum and Zagotta, 1997). Alternatively and more likely (see below), the domain may affect the actual gating machinery, as has been postulated to explain the "molecular brake" (Sansom, 1999) function of the cytoplasmic PAS domain in the HERG

channel (Morais Cabral et al., 1998). The recent observation that pH-dependent channel closure coincides with a structural rearrangement of the NH_2 and COOH termini (Schulte et al., 1998) provides credence for this latter idea. Indeed, the COOH-terminal structure (C308) that undergoes the pH-dependent allosteric change appears to lay in close proximity to the modulatory domain that we have identified (332–351).

While the actual mechanism underlying the COOH-terminal regulatory function remains to be elucidated, our data chiefly point to one particular model. As supported by direct protein–protein interaction studies in Kir1.1 (Koster et al., 1998) and other inwardly rectifying potassium channels (Tinker et al., 1996), the dominant negative behavior of 331X revealed that the COOH-terminal domain (332–391) not only controls open-state occupancy, but is also an important determinant of subunit oligomerization. Such overlapping functions suggest that intersubunit interactions within the COOH terminus may regulate the energetics of channel opening. Accordingly, we propose that disruption of the intersubunit contacts within the COOH-terminal domain alters the quaternary structure of the tetramer in a way that perturbs the stability of the open pore, comparable with the way that oxygen induces an allosteric conformational change in hemoglobin (Perutz et al., 1998).

Considering the similarities in the primary structure of the COOH-terminal domain within the inward-rectifying potassium channel family, the modulatory function of this structure may be more widespread. Within the affected COOH-terminal domain of Kir 1.1 (332–391), the distinct region that is absolutely required for channel function (332–351) exhibits the highest degree of amino acid conservation, sharing ~30% identity with other members of the inward-rectifying channel family. Interestingly, Drain et al. (1998) recently identified a structural determinant of ATP-dependent gating in a distantly related K_{ATP} subunit, Kir 6.2, that lies within this moderately conserved domain. In view of this observation, the extreme COOH-terminal domain may act on conserved gating structure in the inward rectifying potassium channel family.

In summary, we have elucidated the mechanism underlying the functional defect of a particular Kir 1.1a mutant that has been linked with the familial salt wasting nephropathy, Bartter's syndrome. These efforts revealed that a previously unrecognized domain, the extreme COOH terminus, acts as an important modifier of channel gating.

Submitted: 30 March 1999 Revised: 17 September 1999 Accepted: 20 September 1999 Released online: 11 October 1999

REFERENCES

Babenko, A.P., L. Aguilar-Bryan, and J. Bryan. 1998. A view of sur/KIR6.X, K_{ATP} channels. *Annu Rev. Physiol*. 60:667–687.

Bartter, F.C., P. Pronove, J.R. Gill, Jr., and R.C. MacCardle. 1962. Hyperplasia of the juxtaglomerular complex with hyperaldosteronism and hypokalemic alkalosis: a new syndrome. *Am. J. Med*. 33:811–828.

Bleich, M., E. Schlatter, and R. Greger. 1990. The luminal K^+ channel of the thick ascending limb of Henle's loop. *Pflügers Arch*. 415:449–460.

Brejon, M., S. LeMaout, P.A. Welling, and J. Merot. 1999. Processing and transport of the ROMK1 channel is temperature-sensitive. *Biochem. Biophys. Res. Commun*. 261:364–371.

Choe, H., H. Zhou, L.G. Palmer, and H. Sackin. 1997. A conserved cytoplasmic region of ROMK modulates pH sensitivity, conductance and gating. *Am. J. Physiol*. 273:F516–F529.

Choe, H., H. Sackin, and L.G. Palmer. 1998. Permeation and gating of an inwardly rectifying potassium channel: evidence for a variable energy well. *J. Gen. Physiol*. 112:433–446.

Cormack, B.P., R.H. Valdivia, and S. Falkow. 1996. FACS-optimized mutants of the green fluorescent protein (GFP). *Gene*. 173:33–38.

Derst, C., M. Konrad, A. Kockerling, L. Karolyi, G. Deschennes, J. Daut, A. Karschin, and H.W. Seyberth. 1997. Mutations in the ROMK gene in antenatal Bartter syndrome are associated with impaired K^+ channel function. *Biochem. Biophys. Res. Commun*. 203:641–645.

Derst, C., E. Wischmeyer, R. Preisig-Muller, A. Spauschus, M. Konrad, P. Hensen, N. Jeck, H.W. Seyberth, J. Daut, and A. Karschin. 1998. A hyperprostaglandin E syndrome mutation in Kir 1.1 (renal outer medullary potassium) channels reveals a crucial residue for channel function in Kir 1.3 channels. *J. Biol. Chem*. 273: 23884–23891.

Drain, P., L. Li, and J. Wang. 1998. K_{ATP} channel inhibition of ATP requires distinct functional domains of the cytoplasmic C terminus of the pore-forming subunit. *Proc. Natl. Acad. Sci. USA*. 95: 13953–13958.

Fakler, B., J.H. Schultz, J. Yang, U. Schulte, U. Brandle, H.P. Zenner, L.Y. Jan, and J.P. Ruppersberg. 1996. Identification of a titratable lysine residue that determines sensitivity of kidney potassium channels (ROMK) to intracellular pH. *EMBO (Eur. Mol. Biol. Organ.) J*. 15:4093–4099.

Firsov, D., L. Schild, I. Gautschi, A.M. Merillat, E. Schneeberger, and B.C. Rossier. 1996. Cell surface expression of the epithelial Na channel and a mutant causing Liddle syndrome: a quantitative approach. *Proc. Natl. Acad. Sci. USA*. 93:15370–15375.

Frindt, G., and L.G. Palmer. 1989. Low-conductance K channels in apical membrane of rat cortical collecting tubule. *Am. J. Physiol*. 256:F143–F151.

Giebisch, G. 1998. Renal potassium transport: mechanisms and regulation. *Am. J. Physiol*. 274:F817–F833.

Glowatzki, E., G. Fakler, U. Brandle, U. Rexhausen, H.-P. Zenner, J.P. Ruppersberg, and B. Fakler. 1995. Subunit-dependent assembly of inward-rectifier K^+ channels. *Proc. R. Soc. Lond. B Biol. Sci*. 261:251–261.

Guay-Woodford, L.M. 1998. Bartter syndrome: unraveling the pathophysiologic enigma. *Am. J. Med*. 105:151–161.

Hamill, O.P., A. Neher, B. Sakmann, and F.J. Sigworth. 1981. Improved patch-clamp techniques for high-resolution current re-

cording from cells and cell-free membrane patches. *Pflügers Arch.* 391:85–100.

Hebert, S.C., and W.H. Wang. 1997. Structure and function of the low conductance KATP channel, ROMK. *Wien. Klin. Wochenschr.* 109:471–476.

Ho, K., C.G. Nichols, W.J. Lederer, J. Lytton, P.M. Vassilev, M.V. Kanazirska, and S.C. Hebert. 1993. Cloning and expression of an inwardly rectifying ATP-regulated potassium channel. *Nature.* 362:31–38.

Ho, S.N., H.D. Hunt, R.M. Horton, J.K. Pullen, and L.R. Pease. 1989. Site-directed mutagenesis by overlap extension using the polymerase chain reaction. *Gene.* 77:51–59.

Karolyi, L., M. Konrad, A. Kockerling, A. Ziegler, D.K. Zimmerman, B. Roth, C. Wieg, K.-H. Grzeschik, M.C. Kock, H.W. Seyberth, et al. 1997. Mutations in the gene encoding the inwardly-rectifying renal potassium channel, ROMK, cause the antenatal variant of Bartter syndrome: evidence for genetic heterogeneity. *Hum. Mol. Genet.* 6:17–26.

Kohda, Y., W. Ding, E. Phan, I. Housini, J. Wang, R.A. Star, and C.L. Huang. 1998. Localization of the ROMK potassium channel to the apical membrane of distal nephron in rat kidney. *Kidney Int.* 54:1214–1223.

Koster, J.C., K.A. Bentle, C.G. Nichols, and K. Ho. 1998. Assembly of ROMK1 (Kir 1.1a) inward rectifier K^+ channel subunits involves multiple interaction sites. *Biophys. J.* 74:1821–1829.

Krieg, P.A., and D.A. Melton. 1984. Functional messenger RNAs are produced by SP6 *in vitro* transcription of cloned cDNAs. *Nucleic Acids Res.* 12:7057–7070.

Lu, Z., and R. Mackinnon. 1994. A conductance maximum observed in an inward-rectifier potassium channel. *J. Gen. Physiol.* 104:477–486.

MacGregor, G.G., J.Z. Xu, C.M. McNicholas, G. Giebisch, and S.C. Hebert. 1998. Partially active channels produced by PKA site mutation of the cloned renal K^+ channel, ROMK2 (kir1.2). *Am. J. Physiol.* 275:F415–F422.

Mackinnon, R. 1991. Determination of the subunit stoichiometry of a voltage-activated potassium channel. *Nature.* 350:232–235.

McNicholas, C.M., W. Wang, K. Ho, S.C. Hebert, and G. Giebisch. 1994. Regulation of ROMK1 K^+ channel activity involves phosphorylation processes. *Proc. Natl. Acad. Sci. USA.* 91:8077–8081.

McNicholas, C.M., W.B. Guggino, E.M. Schwiebert, S.C. Hebert, G. Giebisch, and M.E. Egan. 1996. Sensitivity of a renal K^+ channel (ROMK2) to the inhibitory sulfonylurea compound glibenclamide is enhanced by coexpression with the ATP-binding cassette transporter cystic fibrosis transmembrane regulator. *Proc. Natl. Acad. Sci. USA.* 93:8083–8088.

McNicholas, C.M., G.G. MacGregor, L.D. Islas, Y. Yang, S.C. Hebert, and G. Giebisch. 1998. pH-dependent modulation of the cloned renal K^+ channel, ROMK. *Am. J. Physiol.* 275:F972–F981.

Mennitt, P.A., J.B. Wade, C.A. Ecelbarger, L.G. Palmer, and G. Frindt. 1997. Localization of ROMK channels in the rat kidney. *J. Am. Soc. Nephrol.* 8:1823–1830.

Methfessel, C., V. Witzemann, T. Takahashi, M. Mishina, S. Numa, and B. Sakmann. 1986. Patch clamp measurements on *Xenopus laevis* oocytes: currents through endogenous channels and implanted acetylcholine receptor and sodium channels. *Pflügers Arch.* 407:577–588.

Morais Cabral, J.H., A. Lee, S.L. Cohen, B.T. Chait, M. Li, and R. Mackinnon. 1998. Crystal structure and functional analysis of the HERG potassium channel N terminus: a eukaryotic PAS domain. *Cell.* 95:649–655.

Nichols, C.G., and A.N. Lopatin. 1997. Inward rectifier potassium channels. *Annu. Rev. Physiol.* 59:171–191.

Palmer, L.G., H. Choe, and G. Frindt. 1997. Is the secretory K channel in the rat CCT ROMK? *Am. J. Physiol.* 273:F404–F410.

Perutz, M.F., A.J. Wilkinson, M. Paoli, and G.G. Dodson. 1998. The stereochemical mechanism of the cooperative effects in hemoglobin revisited. *Annu. Rev. Biophys. Biomol. Struct.* 27:1–34.

Ruknudin, A., D.H. Schulze, S.K. Sullivan, W.J. Lederer, and P.A. Welling. 1998. Novel subunit composition of a renal epithelial K_{ATP} channel. *J. Biol. Chem.* 273:14165–14171.

Sansom, M.S.P. 1999. Structure of a molecular brake. *Curr. Biol.* 9:R173–R175.

Schulte, U., H. Hahn, H. Wiesinger, J.P. Ruppersberg, and B. Fakler. 1998. pH-dependent gating of ROMK (Kir 1.1) channels involves conformational changes in both N and C termini. *J. Biol. Chem.* 273:34575–34579.

Schwalbe, R.A., L. Bianchi, E.A. Accili, and A.M. Brown. 1998. Functional consequences of ROMK mutants linked to antenatal Bartter's syndrome and implications for treatment. *Hum. Mol. Gen*et. 7:975–980.

Sigworth, F.J., and S.M. Sine. 1987. Data transformations for improved display and fitting of single-channel dwell time histograms. *Biophys. J.* 52:1047–1054.

Simon, D.B., F.E. Karet, J.M. Hamdan, A. DiPietro, S.A. Sanjad, and R.P. Lifton. 1996a. Bartter's syndrome, hypokalaemic alkalosis with hypercalciuria, is caused by mutations in the Na-K-2Cl cotransporter NKCC2. *Nat. Genet.* 13:183–188.

Simon, D.B., F.E. Karet, J. Rodriguez-Soriano, J.H. Hamdan, A. DiPietro, H. Trachtman, S.A. Sanjad, and R.P. Lifton. 1996b. Genetic heterogeneity of Bartter's syndrome revealed by mutations in the K^+ channel, ROMK. *Nat. Genet.* 14:152–156.

Simon, D.B., C. Nelson-Williams, M.J. Bia, D. Ellison, F.E. Karet, A.M. Molina, I. Vaara, F. Iwata, H.M. Cushner, M. Koolen, et al. 1996c. Gitelman's variant of Bartter's syndrome, inherited hypokalaemic alkalosis, is caused by mutations in the thiazide-sensitive Na-Cl cotransporter. *Nat. Genet.* 12:24–30.

Taglialatela, M., B.A. Wible, R. Caporaso, and A.M. Brown. 1994. Specification of pore properties by the carboxyl terminus of inwardly rectifying K^+ channels. *Science.* 264:844–847.

Tinker, A., Y.N. Jan, and L.Y. Jan. 1996. Regions responsible for the assembly of inwardly rectifying potassium channels. *Cell.* 87:857–868.

Varnum, M.D., and W.N. Zagotta. 1997. Interdomain interaction underlying activation of cyclic nucleotide-gated channels. *Science.* 278:110–113.

Wang, W.H., A. Schwab, and G. Giebisch. 1990a. Regulation of small-conductance K^+ channel in apical membrane of rat cortical collecting tubule. *Am. J. Physiol.* 259:F494–F502.

Wang, W.H., S. White, J. Geibel, and G. Giebisch. 1990b. A potassium channel in the apical membrane of rabbit thick ascending limb of Henle's loop. *Am. J. Physiol.* 258:F244–F253.

Welling, P.A. 1997. Primary structure and functional expression of a cortical collecting duct K_{ir} channel. *Am. J. Physiol.* 273:F825–F836.

Xu, J.Z., A.E. Hall, L.N. Peterson, M.J. Bienkowski, T.E. Eessalu, and S.C. Hebert. 1997. Localization of the ROMK protein on apical membranes of rat kidney nephron segments. *Am. J. Physiol.* 273:F739–F748.

Xu, Z., Y. Yang, and S.C. Hebert. 1996. Phosphorylation of the ATP-sensitive, inwardly rectifying K^+ channel, ROMK, by cyclic AMP-dependent protein kinase. *J. Biol. Chem.* 271:9313–9319.

Yang, J., Y.N. Jan, and L.Y. Jan. 1995a. Control of rectification and permeation by residues in two distinct domains in an inwardly rectifying K^+ channel. *Neuron.* 14:1047–1054.

Yang, J., Y.N. Jan, and L.Y. Jan. 1995b. Determination of the subunit stoichiometry of an inwardly rectifying potassium channel. *Neuron.* 15:1441–1447.

Yang, X.C., and F. Sachs. 1990. Characterization of stretch-activated ion channels in *Xenopus* oocytes. *J. Physiol.* 431:103–122.